


## RESEARCH ARTICLE

# Altered myelination in youth born with congenital heart disease

Kaitlyn Easson<sup>1,2</sup> | Guillaume Gilbert<sup>3</sup> | Charles V. Rohlicek<sup>4</sup> |  
Christine Saint-Martin<sup>5</sup> | Maxime Descoteaux<sup>6</sup> | Sean C. L. Deoni<sup>7</sup> |  
Marie Brossard-Racine<sup>1,2,8,9</sup> 

<sup>1</sup>Advances in Brain & Child Development (ABCD) Research Laboratory, Research Institute of the McGill University Health Centre, Montreal, Quebec, Canada

<sup>2</sup>Department of Neurology & Neurosurgery, Faculty of Medicine, McGill University, Montreal, Quebec, Canada

<sup>3</sup>MR Clinical Science, Philips Healthcare, Mississauga, Ontario, Canada

<sup>4</sup>Department of Pediatrics, Division of Cardiology, Montreal Children's Hospital, Montreal, Quebec, Canada

<sup>5</sup>Department of Medical Imaging, Division of Pediatric Radiology, Montreal Children's Hospital, Montreal, Quebec, Canada

<sup>6</sup>Sherbrooke Connectivity Imaging Laboratory (SCIL), Université de Sherbrooke, Sherbrooke, Quebec, Canada

<sup>7</sup>Advanced Baby Imaging Lab, Brown University, Providence, Rhode Island, USA

<sup>8</sup>Department of Pediatrics, Division of Neonatology, Montreal Children's Hospital, Montreal, Quebec, Canada

<sup>9</sup>School of Physical & Occupational Therapy, McGill University, Montreal, Quebec, Canada

## Correspondence

Marie Brossard-Racine, Advances in Brain & Child Development (ABCD) Research Laboratory, Research Institute of the McGill University Health Centre, Montreal, QC, Canada.  
Email: [marie.brossardracine@mcgill.ca](mailto:marie.brossardracine@mcgill.ca)

## Funding information

This study was supported by funding from McGill University and the Research Institute of the McGill University Health Centre. At the time of manuscript preparation, Kaitlyn Easson was supported by a Vanier Canada Graduate Scholarship from the Canadian Institutes of

## Abstract

Brain injury and dysmaturation is common in fetuses and neonates with congenital heart disease (CHD) and is hypothesized to result in persistent myelination deficits. This study aimed to quantify and compare myelin content *in vivo* between youth born with CHD and healthy controls. Youth aged 16 to 24 years born with CHD and healthy age- and sex-matched controls underwent brain magnetic resonance imaging including multicomponent driven equilibrium single pulse observation of  $T_1$  and  $T_2$  (mcDESPOt). Average myelin water fraction (MWF) values for 33 white matter tracts, as well as a summary measure of average white matter MWF, the White Matter Myelination Index, were calculated and compared between groups. Tract-average MWF was lower throughout the corpus callosum and in many bilateral association tracts and left hemispheric projection tracts in youth with CHD ( $N = 44$ ) as compared to controls ( $N = 45$ ). The White Matter Myelination Index was also lower in the CHD group. As such, this study provides specific evidence of widespread myelination deficits in youth with CHD, likely representing a long-lasting consequence of early-life brain dysmaturation in this population. This deficient myelination may underlie the frequent neurodevelopmental impairments experienced by CHD survivors and could eventually serve as a biomarker of neuropsychological function.

## KEYWORDS

congenital heart disease, myelination, neurodevelopment, quantitative magnetic resonance imaging

This is an open access article under the terms of the [Creative Commons Attribution-NonCommercial-NoDerivs](https://creativecommons.org/licenses/by-nc-nd/4.0/) License, which permits use and distribution in any medium, provided the original work is properly cited, the use is non-commercial and no modifications or adaptations are made.

© 2022 The Authors. *Human Brain Mapping* published by Wiley Periodicals LLC.

Health Research. Marie Brossard-Racine was supported by a Canada Research Chair in Brain and Child Development.

## 1 | INTRODUCTION

Despite undergoing open-heart surgery during infancy, survivors of complex congenital heart disease (CHD) frequently experience persistent neurodevelopmental impairments (Easson et al., 2019; Latal, 2016) whose precise neural correlates remain unclear. The neurodevelopment of fetuses and neonates with complex CHD is commonly complicated by delayed brain maturation and associated white matter injury (Brossard-Racine et al., 2016; Licht et al., 2009; Miller et al., 2004, 2007), believed to be a consequence of deficient delivery of blood and oxygen to the brain by the malformed heart (Licht et al., 2004; Sun et al., 2015). From the study of animal models, it is understood that a key factor in the neuropathology of CHD is the heightened vulnerability of the pre-myelinating late oligodendrocyte progenitors (preOLs) that predominate in the immature brain to hypoxia-ischemia (Back et al., 2001; Morton et al., 2017). The cascade following hypoxia-ischemia involves acute preOL death, typically manifesting as diffuse white matter injury, followed by sub-acute preOL replenishment and chronic arrested preOL maturation (Back et al., 2001; Morton et al., 2017). The interrupted maturation of these progenitors into mature, myelinating oligodendrocytes could therefore result in long-term disruptions to myelination across the lifespan of CHD survivors. Given the important role of myelin in coordinating efficient signal transmission within the brain (Fries, 2005), myelination deficits could play a role in the neurodevelopmental impairments frequently experienced by individuals with CHD.

Several diffusion tensor imaging studies have previously detected microstructural white matter alterations, represented by lower fractional anisotropy and higher radial diffusivity, in infants (Karmacharya et al., 2018; Miller et al., 2007) and youth (Brewster et al., 2015; Easson et al., 2020; Ehrler et al., 2020; Rivkin et al., 2013; Watson et al., 2018) with CHD. While these findings could reflect low myelination, diffusion tensor imaging metrics are influenced by several other microscopic attributes of white matter, including axon density, diameter, and orientation and membrane permeability (Jones et al., 2013). Neurite orientation dispersion and density imaging, an advanced multi-compartment diffusion modeling technique, has recently been used to uncover reductions in the neurite density index in infants (Karmacharya et al., 2018) and youth (Easson et al., 2020) with CHD. These findings suggest a lower density of axonal packing, which could be the result of disrupted myelination but could also reflect axon loss. Taken together, while these previous diffusion magnetic resonance imaging (MRI) studies provide important evidence of persistent alterations to white matter microstructure across the lifespan of CHD survivors, the extent to which these findings specifically reflect disrupted myelination remains unclear.

For a long time, direct quantification of brain myelination was limited to histological analysis of post-mortem brain tissue (Kinney et al., 2005). Recent advancements in quantitative MRI have allowed for

the development of techniques that provide specific estimates of myelin content *in vivo*. This includes multicomponent relaxation techniques, such as multicomponent driven equilibrium single pulse observation of  $T_1$  and  $T_2$  (mcDESPOT) (Deoni et al., 2013), which allow for the calculation of the myelin water fraction (MWF). MWF is a reliable measure of myelin content, strongly correlated with the gold standard histological measurement of myelination (Laule et al., 2006). mcDESPOT has previously been used to describe trajectories of myelination during typical development (Deoni et al., 2012), as well as myelin alterations in individuals with autism spectrum disorder (Deoni et al., 2015) and mild traumatic brain injury (Spader et al., 2018). However, this promising technique has yet to be applied to investigate the potential long-term disruptions to myelin development in the CHD population. Therefore, the primary objective of this study was to compare white matter myelination, as measured by mcDESPOT-derived MWF values, between adolescents and young adults born with CHD and healthy age- and sex-matched controls. As a secondary objective, we explored associations between myelination and several clinical and neuroanatomical factors.

## 2 | MATERIALS & METHODS

### 2.1 | Participants

Term-born adolescents and young adults aged 16 to 24 years who underwent open-heart surgery involving cardiopulmonary bypass for complex CHD before two years of age were recruited for this cross-sectional study. We first recruited CHD participants from a previous study examining determinants of leisure participation in adolescents with CHD (Dahan-Oliel et al., 2014), and recruited additional participants directly from the pediatric and adult cardiology clinics of the McGill University Health Centre. A group of age- and sex-matched healthy controls were recruited from the community as previously described (Easson et al., 2020). Control participants were considered to be typically developing if they had no history of neurological or developmental conditions and had never received special education or rehabilitation services during childhood or adolescence.

Exclusion criteria for both groups included: preterm birth (<37 weeks gestational age), prior history of brain tumor or malformation, documented traumatic brain injury, cerebral palsy, multi-organ dysmorphic conditions, documented genetic or chromosomal abnormalities, contraindications for MRI, and inability to communicate in English or French. Written informed consent was obtained from participants aged 18 years and older and from the legal guardians of participants aged younger than 18 years. Participants younger than 18 years also provided written informed assent. This study was approved by the Pediatric Research Ethics Board of the McGill University Health Centre. Participant recruitment and data collection occurred from March 2016 to December 2019.

## 2.2 | MRI acquisition

Participants completed a single study visit at the McGill University Health Centre involving a brain MRI on a 3T MRI System (Achieva X, Philips Healthcare, Best, The Netherlands) using a 32-channel head coil. The MRI protocol included T1-weighted, high angular resolution diffusion imaging (HARDI), and mcDESPOT acquisitions.

The T1-weighted anatomical image was acquired with a turbo field echo pulse sequence (TR = 8.1 ms, TE = 3.7 ms, TI = 1010 ms, flip angle = 8°, voxel size = 1.00 × 1.00 × 1.00 mm<sup>3</sup>). All anatomical images from both groups were inspected for overt brain abnormalities by an experienced neuroradiologist (C.S.M.), who was blinded to the medical histories of the participants.

The HARDI acquisition (TR = 9400 ms, TE = 78 ms, flip angle = 90°, voxel size = 2.00 × 2.04 × 2.00 mm<sup>3</sup>) was comprised of a non-diffusion-weighted sequence ( $b = 0$  s/mm<sup>2</sup>) with reversed phase encoding, as well as two single-shell HARDI sequences ( $b = 700$  s/mm<sup>2</sup> and 30 directions;  $b = 2000$  s/mm<sup>2</sup> and 60 directions), which each also included a non-diffusion-weighted volume ( $b = 0$  s/mm<sup>2</sup>).

The mcDESPOT acquisition included a series of 10 spoiled gradient recalled echo (SPGR) sequences (TR = 6.7 ms, TE = 3.7 ms, voxel size = 1.67 × 1.67 × 1.70 mm<sup>3</sup>) covering flip angles from 2° to 18° and eight balanced steady-state free precession (bSSFP) sequences (TR = 6.8 ms, TE = 3.4 ms, voxel size = 1.67 × 1.67 × 1.70 mm<sup>3</sup>) covering flip angles from 12° to 70°. The bSSFP sequences were acquired at two phase-cycling increments (0° and 180°) to enable the correction of main magnetic field ( $B_0$ ) inhomogeneity effects (Deoni, 2011). The mcDESPOT acquisition also included an inversion recovery SPGR (IR-SPGR) sequence (TR = 6.5 ms, TE = 3.2 ms, TI = 450 ms, flip angle = 5°, voxel size = 1.67 × 1.67 × 1.70 mm<sup>3</sup>) to enable the correction of transmit magnetic field ( $B_1$ ) inhomogeneity effects (Deoni, 2011).

## 2.3 | MRI processing

The T1-weighted and diffusion-weighted images were processed using the TractoFlow pipeline (Di Tommaso et al., 2017; Kurtzer et al., 2017; Theaud et al., 2020) and a modified version of RecoBundles (Garyfallidis et al., 2018) in order to extract a total of 33 white matter tracts, including association tracts, projection tracts, cerebellar tracts, and subdivisions of the corpus callosum, for each participant. The TractoFlow pipeline output also includes a pre-processed T1-weighted reference image, whole-brain mask, and tissue masks (i.e., white matter, gray matter, and cerebrospinal fluid masks) in diffusion space for each participant. These data processing steps have previously been described in detail by our group (Easson et al., 2020). In parallel, the data from the mcDESPOT acquisition were processed to generate three-dimensional maps of MWF for each participant as previously described (Deoni et al., 2013). Afterwards, each participant's MWF map was linearly registered to their diffusion-space T1-weighted reference image to ensure that

subjects' MWF maps were properly aligned with their white matter tracts.

We first calculated tract-specific estimates of MWF, which may be more sensitive in detecting group differences and associations with clinical and neuroanatomical risk factors. To accomplish this, the extracted white matter tracts and MWF maps of the participants were used to perform tractometry, involving the calculation of an average MWF value for each white matter tract and white matter tract volumes for each participant (Cousineau et al., 2017). In order to explore the value of simple post-processing techniques that may be more easily transferable to the clinical setting, we also calculated a summary measure of white matter myelination for each participant separately. This summary measure will herein be referred to as the White Matter Myelination Index. To accomplish this, each participant's diffusion-space whole-brain mask and tissue masks were used to calculate a "safe" white matter mask, as previously described (Dumont et al., 2019). This mask conservatively delineates the whole-brain white matter, eliminating voxels that may be contaminated by gray matter or cerebrospinal fluid near tissue boundaries or ventricles. The White Matter Myelination Index was then calculated as the mean value of MWF within the "safe" white matter mask for each participant.

All raw and pre-processed T1-weighted, diffusion-weighted, SPGR, IR-SPGR, and bSSFP images, final MWF maps, and "safe" white matter masks underwent visual inspection for image quality and artifacts. Participants whose images failed any of these quality control steps were excluded from statistical analyses. Furthermore, each extracted white matter tract was visually inspected to ensure anatomical accuracy and robustness. Individual tracts that failed quality inspection were excluded from subsequent statistical analyses.

## 2.4 | Clinical data collection

On the day of the study visit, the height and weight of each participant was measured to allow for calculation of their body mass index. The Hollingshead Four-Factor Index (Hollingshead, 2011) was used to quantify participants' socioeconomic status based on the education and employment status of their parents. Following the study visit, the medical records of all CHD participants were reviewed to collect clinical data, including their specific CHD diagnosis and various perinatal clinical factors including the number of open-heart surgeries and cardiac catheterizations, age at first open-heart surgery, bypass and aortic cross clamp duration at first open-heart surgery, and use and duration of deep-hypothermic circulatory arrest at first open-heart surgery.

## 2.5 | Neurodevelopmental data collection

CHD participants were screened for cognitive deficit based on an intelligence quotient (IQ) threshold of <70, as previously described by our group in detail (Fontes et al., 2019). For the participants recruited

through the previous research study (Dahan-Oliel et al., 2014), records of a previous IQ evaluation using the Leiter International Performance Scale - Revised (Leiter - R) (Roid & Miller, 2011) were available. Newly recruited participants were assessed with the Wechsler Abbreviated Scale of Intelligence - 1st Edition (WASI) (Wechsler, 1999). Both measures are valid and reliable concise evaluations of IQ (Axelrod, 2002; Hooper & Bell, 2006; Ryan et al., 2003; Saklofske et al., 2000). Participants were identified as having a cognitive deficit on the basis of a Leiter - R brief IQ score <70 or a WASI Full Scale-4 IQ score <70. Information about confirmed diagnosis of attention deficit hyperactivity disorder (ADHD) was collected from self-report questionnaires administered to CHD participants or one of their parents during the study visit.

## 2.6 | Statistical analysis

Descriptive statistics were first used to compare the two groups in terms of their individual characteristics, which included age, sex, body mass index, and socioeconomic status. Distribution normality was evaluated using Shapiro-Wilk tests. Between-group comparisons of individual characteristics were performed using two-sample *t*-tests and Mann-Whitney U-tests for continuous variables and  $\chi^2$  tests and Fisher exact tests for categorical variables.

Tract-average MWF values and White Matter Myelination Index values were compared between the CHD and control groups using a series of non-parametric permutation *t*-tests (Nichols & Holmes, 2002). In order to examine the relationship between CHD physiology and MWF measures, CHD participants were categorized into diagnostic sub-groups to be compared to the control group with a series of non-parametric permutation *t*-tests. A diagnostic sub-group was defined for each physiology with  $\geq 10$  participants. The remaining participants were categorized into pooled single-ventricle or two-ventricle sub-groups. The relationship between MWF measures and other clinical, neuroanatomical, and neurodevelopmental variables were examined using non-parametric permutation correlation tests (Di Ciccio & Romano, 2017) for continuous variables (e.g., bypass duration, socioeconomic status) and non-parametric permutation *t*-tests for dichotomous variables (e.g., presence of overt cerebral abnormality, diagnosis of ADHD). Partial correlations controlling for age were used to examine the relationship between tract-average MWF and corresponding tract volume, to account for the ongoing

maturation of white matter in adolescence and adulthood (Lebel & Beaulieu, 2011). All permutations tests sampled the null distribution of the test statistic with 10,000 permutations. Correction for multiple comparisons across white matter tracts was done using the false discovery rate method, setting a threshold of statistical significance of  $q < 0.05$ . Cohen's *d* statistic was used to describe effect size for group comparisons.

## 3 | RESULTS

### 3.1 | Participant characteristics

A total of 53 adolescents and young adults with CHD and 53 age- and sex-matched controls were enrolled in this study. One participant in each group elected to terminate the MRI session prematurely after experiencing personal discomfort in the MRI machine, while eight CHD and seven control participants were subsequently excluded due to poor quality of the raw or processed images. Therefore, complete data of good quality from 44 CHD and 45 control participants were included in the analyses. Excluded participants did not differ significantly from included participants in terms of age, sex, body mass index, socioeconomic status, or presence of cognitive deficit or ADHD diagnosis. The individual characteristics of the final study sample are outlined in Table 1.

The CHD group was comprised of seven participants with a single-ventricle physiology (double inlet left ventricle:  $n = 2$ ; hypoplastic left heart syndrome:  $n = 1$ ; pulmonary atresia with intact ventricular septum:  $n = 3$ ; tricuspid atresia:  $n = 1$ ), 15 participants with dextro-transposition of the great arteries, 12 participants with tetralogy of Fallot, and 10 participants with another type of two-ventricle physiology (double outlet right ventricle:  $n = 2$ ; Ebstein's anomaly:  $n = 1$ ; total anomalous pulmonary venous connection:  $n = 2$ ; truncus arteriosus type I:  $n = 1$ ; ventricular septal defect:  $n = 4$ ). Further clinical characteristics of the CHD group are presented in Table 2.

Clinically significant cerebral abnormalities, likely from an acquired origin, were observed in 11.4% (5/44) of youth with CHD and 2.2% (1/45) of control youth. This difference was not statistically significant ( $p = 0.110$ ). The observed abnormalities were all mild in severity. These abnormalities included: one CHD participant with cystic dilation of the perivascular spaces; one CHD participant with notable sequelae of periventricular white matter injury; two CHD

	CHD (N = 44)	Control (N = 45)	<i>p</i> value
Age (years)	20.0 [16.3–24.1]	20.1 [16.8–24.2]	.430
Sex			.927
Female	25 (56.8%)	26 (57.8%)	
Male	19 (43.2%)	19 (42.2%)	
Body mass index	21.9 [17.3–40.0]	22.6 [18.6–33.8]	.305
Socioeconomic status score	39.9 $\pm$ 12.4	50.5 $\pm$ 10.3	<.001

**TABLE 1** Participants' individual characteristics

Note: Descriptive statistics are provided as mean  $\pm$  SD for normally distributed continuous variables, median [range] for non-normally distributed continuous variables, and *n* (%) for categorical variables.

**TABLE 2** Clinical characteristics of the CHD group

	CHD (median [range] or <i>n</i> (%))
CHD physiology	
Single-ventricle physiology	7 (15.9%)
Dextro-transposition of the great arteries	15 (34.1%)
Tetralogy of Fallot	12 (27.3%)
Other two-ventricle physiology	10 (22.7%)
Number of OHS	1 [1–4]
Number of cardiac catheterizations	1.5 [0–5]
Age at 1 <sup>st</sup> OHS (days)	35 [0–702]
Bypass duration, 1 <sup>st</sup> OHS (min)	129.5 [61–292]
Aortic cross clamp duration, 1 <sup>st</sup> OHS (min)	74 [23–162]
Use of DHCA, 1 <sup>st</sup> OHS	18 (47.4%)
DHCA duration, 1 <sup>st</sup> OHS (min)	11 [0–52]
Cognitive deficit (IQ < 70)	2 [4.5%]
ADHD diagnosis	5 [11.4%]

Note: Descriptive statistics are provided as mean ± SD for normally distributed continuous variables, median [range] for non-normally distributed continuous variables, and *n* (%) for categorical variables. Missing variables are excluded from reported percentages (%). Abbreviations: ADHD, attention deficit hyperactivity disorder; DHCA, deep hypothermic circulatory arrest; IQ, intelligence quotient; OHS, open-heart surgery.

participants with susceptibility artifact, likely representing blood deposition or calcification; and one CHD participant and one control participant with periventricular heterotopia. The CHD participants presenting with cerebral abnormalities on conventional MRI all had two-ventricle cardiac physiologies, representing a heterogeneous collection of specific diagnoses.

### 3.2 | Group comparisons of MWF

Between-group comparisons of tract-average MWF are outlined in Table 3 and Figure 1. Compared to control participants, youth with CHD had significantly lower MWF in many association tracts, including the bilateral arcuate fasciculus, left cingulum, bilateral inferior frontal occipital fasciculus, bilateral inferior longitudinal fasciculus, and bilateral superior longitudinal fasciculus I, II, and III. Youth with CHD also presented with lower MWF in the projection tracts in the left hemisphere, namely the left corona radiata, left corticospinal tract, and left optic radiation, with no significant differences in the right hemisphere projection tracts. Finally, youth with CHD had significantly lower MWF in all extracted subdivisions of the corpus callosum. There were no significant differences between the two groups with respect to MWF in the cerebellar tracts. Moreover, the White Matter Myelination Index was significantly lower (Figure 2a;  $p < .001$ ,  $d = 1.03$ ) in the CHD group (mean ± SD = 0.206 ± 0.009) as compared to the control group (mean ± SD = 0.215 ± 0.009).

### 3.3 | Association of MWF with clinical factors

Comparisons of tract-average MWF between CHD diagnostic subgroups and the control group are outlined in Table 4. Compared to controls, tract-average MWF was lower in youth with single-ventricle physiologies in 27 white matter tracts, including many projection and association tracts, often bilaterally, all sub-divisions of the corpus callosum, and the middle cerebellar peduncle. Tract-average MWF was lower in youth with dextro-transposition of the great arteries in four left hemisphere association tracts and two corpus callosum sub-divisions. There were no differences in tract-average MWF between youth with tetralogy of Fallot and control participants that survived correction for multiple comparisons. The remaining group of other two-ventricle physiologies presented with lower MWF in 18 white matter tracts, mostly localized to association tracts and central corpus callosum sub-divisions, as well as the left optic radiation.

The White Matter Myelination Index was also significantly lower in youth with single-ventricle physiologies ( $d = 1.93$ ,  $p < .001$ ), youth with dextro-transposition of the great arteries ( $d = 0.865$ ,  $p = .005$ ), and youth with other two-ventricle physiologies ( $d = 1.33$ ,  $p < .001$ ), but not in youth with tetralogy of Fallot, compared to control participants (Figure 2b).

Neither tract-average MWF in any tract nor the White Matter Myelination Index were significantly correlated with socioeconomic status, body mass index, or any of the other clinical variables examined.

### 3.4 | Association of MWF with neuroanatomical factors

Neither tract-average MWF in any tract nor the White Matter Myelination Index were significantly associated with the presence of overt cerebral abnormalities in the CHD or control groups. In the control group, tract-average MWF and tract volume were positively correlated in the left ( $r = 0.527$ ,  $q = 0.036$ ) and right ( $r = 0.535$ ,  $q = 0.036$ ) uncinate fasciculus. There were no significant correlations between tract-average MWF and corresponding tract volume in the CHD group.

### 3.5 | Association of MWF with neurodevelopmental factors

Neither tract-average MWF in any tract nor the White Matter Myelination Index were significantly associated with the presence of cognitive deficit or ADHD diagnosis.

## 4 | DISCUSSION

In this first study to implement mcDESPOT to quantify myelination in individuals with CHD, our results confirm the presence of widespread deficits in the myelination of many white matter tracts, as measured

**TABLE 3** Comparison of tract-average MWF between CHD and control groups

	CHD (mean ± SD)	Control (mean ± SD)	q value	d value
<b>Association tracts</b>				
AF (L)	0.213 ± 0.010	0.221 ± 0.008	<b>&lt;0.001</b>	1.00
AF (R)	0.218 ± 0.007	0.222 ± 0.008	<b>0.010</b>	0.613
CG (L)	0.203 ± 0.012	0.212 ± 0.015	<b>0.006</b>	0.654
CG (R)	0.206 ± 0.011	0.211 ± 0.016	0.077	0.382
IFOF (L)	0.206 ± 0.010	0.217 ± 0.008	<b>&lt;0.001</b>	1.18
IFOF (R)	0.204 ± 0.010	0.212 ± 0.010	<b>0.003</b>	0.778
ILF (L)	0.217 ± 0.009	0.225 ± 0.008	<b>0.001</b>	0.975
ILF (R)	0.214 ± 0.009	0.221 ± 0.010	<b>0.001</b>	0.724
SLF I (L)	0.207 ± 0.010	0.217 ± 0.010	<b>&lt;0.001</b>	1.03
SLF I (R)	0.210 ± 0.009	0.216 ± 0.010	<b>0.004</b>	0.687
SLF II (L)	0.206 ± 0.009	0.216 ± 0.009	<b>&lt;0.001</b>	1.07
SLF II (R)	0.212 ± 0.008	0.216 ± 0.009	<b>0.034</b>	0.494
SLF III (L)	0.212 ± 0.011	0.220 ± 0.010	<b>&lt;0.001</b>	0.792
SLF III (R)	0.221 ± 0.007	0.225 ± 0.010	<b>0.038</b>	0.463
UF (L)	0.172 ± 0.015	0.179 ± 0.015	0.059	0.437
UF (R)	0.174 ± 0.014	0.180 ± 0.015	0.060	0.414
<b>Corpus callosum</b>				
Rostrum	0.219 ± 0.010	0.224 ± 0.009	<b>0.014</b>	0.579
Genu (A)	0.230 ± 0.007	0.237 ± 0.007	<b>&lt;0.001</b>	0.994
Genu (P)	0.221 ± 0.008	0.230 ± 0.007	<b>&lt;0.001</b>	1.21
Rostral body	0.211 ± 0.009	0.220 ± 0.009	<b>&lt;0.001</b>	0.939
Mid-body (A)	0.206 ± 0.009	0.214 ± 0.011	<b>0.003</b>	0.769
Mid-body (P)	0.200 ± 0.010	0.209 ± 0.011	<b>&lt;0.001</b>	0.826
Isthmus	0.198 ± 0.013	0.206 ± 0.013	<b>0.010</b>	0.610
Splenium	0.206 ± 0.010	0.212 ± 0.013	<b>0.020</b>	0.533
<b>Projection tracts</b>				
CR (L)	0.189 ± 0.011	0.196 ± 0.011	<b>0.005</b>	0.626
CR (R)	0.190 ± 0.010	0.195 ± 0.011	0.051	0.441
CST (L)	0.185 ± 0.012	0.191 ± 0.012	<b>0.026</b>	0.515
CST (R)	0.189 ± 0.011	0.194 ± 0.011	0.060	0.420
OR (L)	0.212 ± 0.009	0.219 ± 0.009	<b>0.003</b>	0.703
OR (R)	0.212 ± 0.009	0.216 ± 0.010	0.057	0.427
<b>Cerebellar tracts</b>				
SCP (L)	0.156 ± 0.015	0.159 ± 0.017	0.445	0.163
SCP (R)	0.157 ± 0.017	0.161 ± 0.018	0.236	0.260
MCP	0.183 ± 0.019	0.190 ± 0.015	0.068	0.409

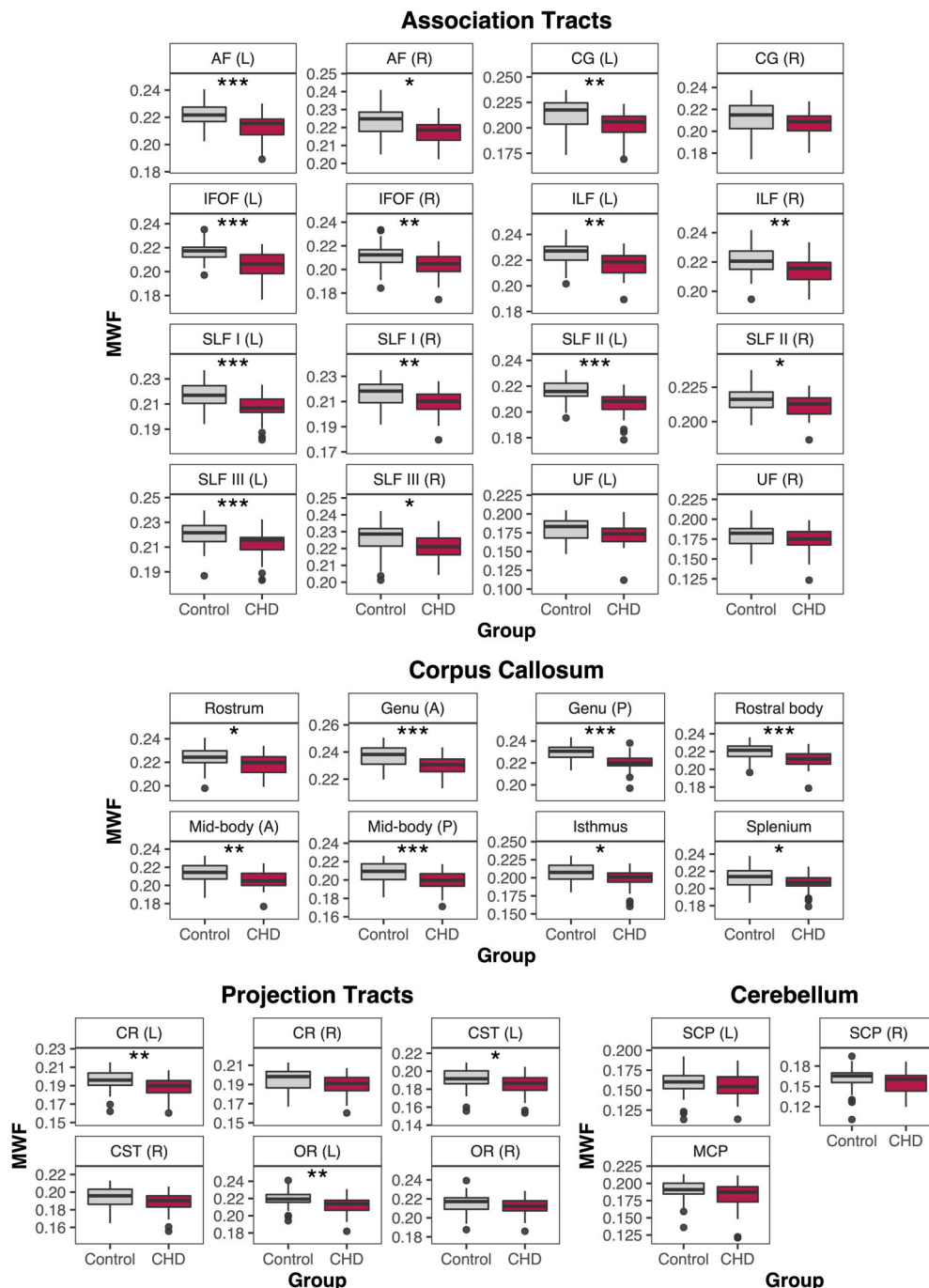
Note: Significant *q* values at a threshold of *q* < 0.05 are indicated in bold font.

Abbreviations: A, anterior; AF, arcuate fasciculus; CG, cingulum; CR, corona radiata; CST, corticospinal tract; IFOF, inferior frontal occipital fasciculus; ILF, inferior longitudinal fasciculus; L, left; MCP, middle cerebellar peduncle; OR, optic radiation; P, posterior; SCP, superior cerebellar peduncle; SLF, superior longitudinal fasciculus; UF, uncinate fasciculus.

by MWF. As such, this work builds upon previous diffusion MRI studies of the CHD population, suggesting a specific role of deficient myelination in the microstructural white matter alterations frequently reported in this population. In particular, analysis of tract-average MWF values revealed that MWF was lower in youth born with complex CHD as compared to healthy peers throughout the corpus

callosum, in many association tracts, often bilaterally, and in the left hemisphere projection tracts. The White Matter Myelination Index was also significantly lower in the CHD group, suggesting that the widespread myelination deficits in youth with CHD are prominent enough to be detected by a simple global summary measure. Overall, our findings suggest that the brain dysmaturation previously

**FIGURE 1** Comparison of tract-average MWF between CHD and control groups. A, anterior; AF, arcuate fasciculus; CG, cingulum; CR, corona radiata; CST, corticospinal tract; IFOF, inferior frontal occipital fasciculus; ILF, inferior longitudinal fasciculus; L, left; MCP, middle cerebellar peduncle; OR, optic radiation; P, posterior; R, right; SCP, superior cerebellar peduncle; SLF, superior longitudinal fasciculus; UF, uncinate fasciculus. \* $q < 0.05$ , \*\* $q < 0.01$ , \*\*\* $q < 0.001$



described in fetuses and neonates with CHD persists throughout adolescence and early adulthood.

#### 4.1 | Enduring myelination deficits in CHD survivors

Brain injury and delayed brain development, as characterized by smaller volumetric growth and altered microstructural and metabolic maturation (Licht et al., 2009; Limperopoulos et al., 2010; Miller et al., 2007), are common in fetuses and neonates with CHD and are

believed be consequences of abnormalities in cerebral blood flow and oxygenation (Licht et al., 2004; Sun et al., 2015). However, longitudinal prospective imaging studies that extend beyond the perioperative period are needed, particularly once cerebral hemodynamics have been fully or partially restored after cardiac surgery, to inform on the evolution of these brain abnormalities. Given the particular vulnerability of the oligodendrocyte lineage to cerebral hypoxia-ischemia, the maturation of white matter tracts, including their myelination, are of particular interest.

Our results are in line with the hypothesized long-term impact of early-life brain injury and dysmaturation on the subsequent myelin

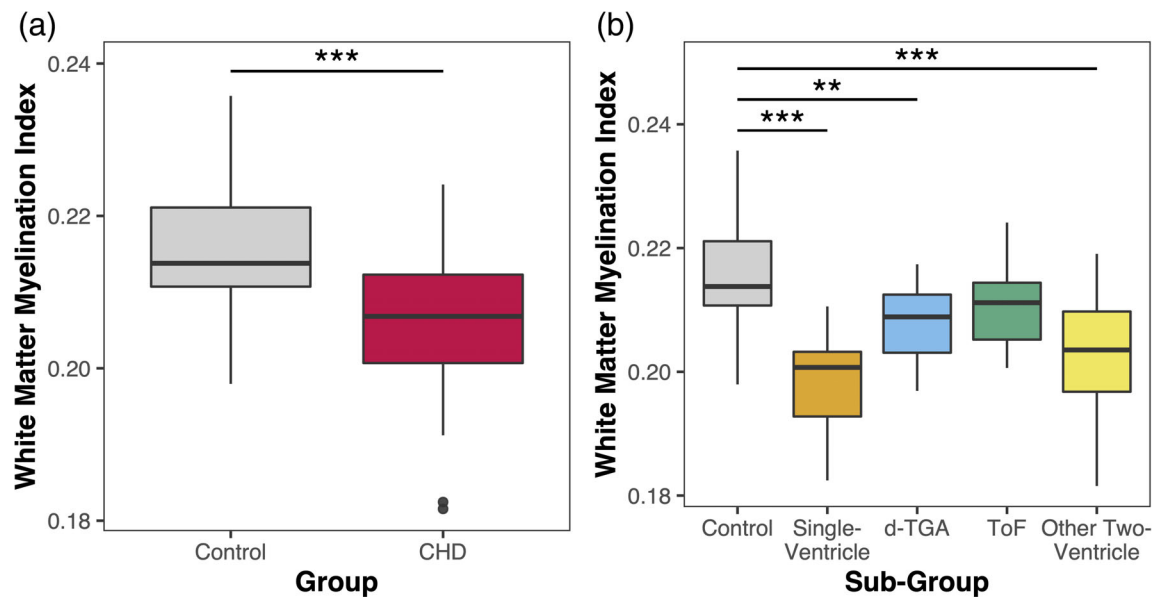


**FIGURE 2** Group and sub-group comparisons of the White Matter Myelination Index. (a) Comparison of the White Matter Myelination Index between CHD and control groups. (b) Comparisons of the White Matter Myelination Index between CHD diagnostic sub-groups and control group. d-TGA, dextro-transposition of the great arteries; ToF, tetralogy of Fallot.  $**p < .01$ ,  $***p < .001$

development of CHD survivors. Given that perinatal white matter injury is believed to play a role in the proposed mechanism of myelination deficits in the CHD population (Morton et al., 2017), it may seem surprising that only one CHD participant presented with sequelae of periventricular white matter injury on conventional MRI, despite our widespread observations of pronounced myelination deficits. However, perinatal brain injuries in infants with CHD have previously been observed to resolve on conventional MRI over time (Mahle et al., 2002), and therefore, may no longer be visible during adolescence. We hypothesize that perinatal white matter injuries may be predictive of later myelination deficits in the CHD population during adolescence and young adulthood. Unfortunately, considering that neonatal imaging was not collected in our CHD cohort, this hypothesis remains speculative for the moment and needs to be confirmed in future longitudinal studies connecting neonatal imaging with brain maturation in childhood and adolescence.

Previous cross-sectional studies have employed diffusion tensor imaging to detect altered white matter microstructure in youth with CHD when compared to healthy peers (Brewster et al., 2015; Easson et al., 2020; Ehrler et al., 2020; Rivkin et al., 2013; Watson et al., 2018). In several of these prior studies, findings of lower fractional anisotropy were more regionally restricted than the present findings of lower MWF (Brewster et al., 2015; Easson et al., 2020; Rivkin et al., 2013). Notably, in our previous diffusion MRI study in this cohort of youth with CHD, we found only small, isolated clusters of voxels of lower fractional anisotropy in the CHD group, with no differences at the tract-average level (Easson et al., 2020), in stark contrast to our current widespread observations of lower tract-average MWF in the cohort. This could be explained by the greater specificity of MWF for myelin content, as various other cellular factors that influence water diffusion could counteract the impact of myelination

deficits on fractional anisotropy and other diffusion tensor imaging metrics (Jones et al., 2013). This direct comparison suggests that specific MRI markers of myelination, such as MWF, are likely more sensitive in detecting the true extent of white matter dysmaturation in CHD survivors than traditional diffusion tensor imaging metrics. Furthermore, MWF measures were not associated with the presence of overt cerebral abnormalities or white matter tract volumes in the CHD group, confirming that conventional and volumetric MRI approaches are likely not sensitive to myelination deficits in this population.

Our results support the eventual added value of incorporating simple measures of myelination into the routine clinical care of the CHD population and other clinical populations of relevance. Nevertheless, it should be noted that the mcDESPOT acquisition and computational processing time required to estimate MWF currently hinder the incorporation of mcDESPOT into routine clinical practice. Regardless, mcDESPOT has improved time efficiency compared to other multicomponent relaxation techniques, allowing for whole-brain acquisitions in a clinically feasible time, making mcDESPOT an ideal candidate for eventual clinical use (Deoni et al., 2013). Future studies should aim to continue to build atlases of norm references of MWF across the lifespan (Dvorak et al., 2021; Morris et al., 2020) that could be used as a reference for clinicians to detect myelination deficits in individuals from various clinical populations, including patients with CHD.

## 4.2 | Myelination and cardiac defect severity

CHD refers to a heterogeneous group of cardiac defects, which can be broadly categorized into single-ventricle and two-ventricle



TABLE 4 Comparison of tract-average MWF between controls and CHD diagnosis sub-groups

	Single-ventricle (N = 7)		d-TGA (N = 15)		Tetralogy of Fallot (N = 12)		Other two-ventricle (N = 10)					
	Mean ± SD	q value	d value	q value	d value	q value	Mean ± SD	q value	d value			
<b>Association tracts</b>												
AF (L)	0.205 ± 0.011	<b>0.001</b>	1.93	0.214 ± 0.009	<b>0.020</b>	0.963	0.217 ± 0.005	0.372	0.540	0.210 ± 0.012	<b>0.005</b>	1.26
AF (R)	0.215 ± 0.007	<b>0.040</b>	0.944	0.219 ± 0.006	0.301	0.398	0.221 ± 0.007	0.761	0.215	0.214 ± 0.007	<b>0.012</b>	1.04
CG (L)	0.193 ± 0.013	<b>0.012</b>	1.29	0.204 ± 0.012	0.165	0.580	0.208 ± 0.009	0.687	0.314	0.204 ± 0.014	0.173	0.560
CG (R)	0.197 ± 0.011	<b>0.040</b>	0.942	0.207 ± 0.010	0.423	0.294	0.212 ± 0.008	0.833	-0.094	0.203 ± 0.010	0.175	0.526
IFOF (L)	0.203 ± 0.013	<b>0.005</b>	1.48	0.209 ± 0.007	<b>0.033</b>	0.981	0.208 ± 0.011	0.101	0.985	0.202 ± 0.008	<b>0.005</b>	1.78
IFOF (R)	0.202 ± 0.014	0.059	0.897	0.207 ± 0.007	0.222	0.532	0.205 ± 0.011	0.284	0.700	0.201 ± 0.009	<b>0.009</b>	1.12
ILF (L)	0.215 ± 0.012	<b>0.021</b>	1.19	0.219 ± 0.007	0.074	0.751	0.217 ± 0.011	0.101	0.943	0.214 ± 0.008	<b>0.005</b>	1.33
ILF (R)	0.212 ± 0.009	<b>0.046</b>	0.896	0.216 ± 0.007	0.165	0.555	0.214 ± 0.011	0.259	0.679	0.213 ± 0.010	<b>0.042</b>	0.835
SLF I (L)	0.199 ± 0.009	<b>0.001</b>	1.88	0.209 ± 0.009	<b>0.033</b>	0.840	0.212 ± 0.006	0.372	0.563	0.205 ± 0.011	<b>0.005</b>	1.25
SLF I (R)	0.204 ± 0.008	<b>0.011</b>	1.24	0.210 ± 0.009	0.124	0.634	0.215 ± 0.007	0.831	0.135	0.207 ± 0.011	<b>0.036</b>	0.928
SLF II (L)	0.199 ± 0.011	<b>0.001</b>	1.92	0.207 ± 0.008	<b>0.013</b>	1.04	0.211 ± 0.006	0.353	0.613	0.205 ± 0.012	<b>0.008</b>	1.21
SLF II (R)	0.209 ± 0.005	<b>0.045</b>	0.912	0.213 ± 0.008	0.271	0.432	0.216 ± 0.007	0.969	-0.016	0.209 ± 0.010	<b>0.038</b>	0.860
SLF III (L)	0.205 ± 0.012	<b>0.005</b>	1.52	0.213 ± 0.011	0.091	0.728	0.217 ± 0.004	0.687	0.305	0.208 ± 0.014	<b>0.022</b>	1.09
SLF III (R)	0.216 ± 0.008	<b>0.046</b>	0.924	0.223 ± 0.007	0.423	0.266	0.225 ± 0.007	0.848	0.066	0.218 ± 0.007	0.061	0.764
UF (L)	0.163 ± 0.025	0.052	0.934	0.176 ± 0.011	0.592	0.171	0.176 ± 0.015	0.761	0.188	0.168 ± 0.008	0.070	0.751
UF (R)	0.167 ± 0.022	0.070	0.813	0.179 ± 0.010	0.819	0.074	0.177 ± 0.016	0.760	0.229	0.169 ± 0.006	<b>0.043</b>	0.802
<b>Projection tracts</b>												
CR (L)	0.180 ± 0.007	<b>0.006</b>	1.39	0.190 ± 0.012	0.262	0.454	0.192 ± 0.009	0.687	0.325	0.188 ± 0.012	0.104	0.694
CR (R)	0.183 ± 0.008	<b>0.021</b>	1.11	0.192 ± 0.011	0.423	0.282	0.194 ± 0.007	0.831	0.121	0.189 ± 0.013	0.175	0.544
CST (L)	0.176 ± 0.007	<b>0.008</b>	1.32	0.187 ± 0.012	0.363	0.344	0.189 ± 0.009	0.760	0.240	0.185 ± 0.013	0.175	0.522
CST (R)	0.183 ± 0.007	<b>0.024</b>	1.05	0.191 ± 0.013	0.423	0.274	0.192 ± 0.007	0.802	0.163	0.188 ± 0.014	0.189	0.504
OR (L)	0.207 ± 0.013	<b>0.021</b>	1.14	0.214 ± 0.004	0.217	0.502	0.214 ± 0.010	0.443	0.493	0.210 ± 0.009	<b>0.025</b>	0.937
OR (R)	0.207 ± 0.009	0.052	0.865	0.214 ± 0.005	0.423	0.264	0.214 ± 0.009	0.760	0.219	0.210 ± 0.011	0.175	0.532
<b>Corpus callosum</b>												
Rostrum	0.208 ± 0.009	<b>0.001</b>	1.73	0.220 ± 0.010	0.316	0.392	0.222 ± 0.008	0.760	0.236	0.220 ± 0.009	0.194	0.494
Genu (A)	0.225 ± 0.008	<b>0.001</b>	1.60	0.232 ± 0.008	0.103	0.686	0.231 ± 0.007	0.101	0.878	0.229 ± 0.006	<b>0.005</b>	1.18
Genu (P)	0.216 ± 0.009	<b>0.001</b>	1.91	0.222 ± 0.007	<b>0.013</b>	1.11	0.224 ± 0.008	0.170	0.815	0.219 ± 0.007	<b>0.005</b>	1.50
Rostral body	0.203 ± 0.012	<b>0.001</b>	1.84	0.212 ± 0.008	<b>0.034</b>	0.873	0.217 ± 0.007	0.687	0.349	0.209 ± 0.008	<b>0.008</b>	1.21
Mid-body (A)	0.196 ± 0.010	<b>0.001</b>	1.73	0.208 ± 0.009	0.165	0.558	0.211 ± 0.008	0.687	0.301	0.205 ± 0.007	<b>0.031</b>	0.904
Mid-body (P)	0.189 ± 0.010	<b>0.001</b>	1.81	0.203 ± 0.010	0.165	0.576	0.204 ± 0.008	0.443	0.487	0.199 ± 0.010	<b>0.031</b>	0.943

(Continues)

TABLE 4 (Continued)

	Single-ventricle (N = 7)		d-TGA (N = 15)		Tetralogy of Fallot (N = 12)		Other two-ventricle (N = 10)	
	Mean ± SD	q value	Mean ± SD	q value	Mean ± SD	q value	Mean ± SD	q value
Isthmus	0.183 ± 0.015	<b>0.001</b>	0.202 ± 0.008	0.363	0.205 ± 0.006	0.831	0.195 ± 0.015	0.062
Splenium	0.197 ± 0.013	<b>0.018</b>	0.207 ± 0.006	0.271	0.211 ± 0.009	0.831	0.204 ± 0.012	0.130
Cerebellar tracts								
SCP (L)	0.151 ± 0.011	0.232	0.157 ± 0.016	0.702	0.157 ± 0.014	0.831	0.158 ± 0.017	0.896
SCP (R)	0.154 ± 0.015	0.331	0.158 ± 0.020	0.592	0.155 ± 0.016	0.687	0.159 ± 0.017	0.708
MCP	0.176 ± 0.012	<b>0.046</b>	0.184 ± 0.023	0.352	0.187 ± 0.012	0.761	0.182 ± 0.025	0.217
				0.376				0.478

Note: Presented q and d values were computed in comparison to the control group (N = 45; descriptive statistics presented in Table 3). Significant q values at a threshold of  $q < 0.05$  are indicated in bold font. Abbreviations: A, anterior; AF, arcuate fasciculus; CG, cingulum; CR, corona radiata; CST, corticospinal tract; d-TGA, dextro-transposition of the great arteries; IFOF, inferior frontal occipital fasciculus; ILF, inferior longitudinal fasciculus; L, left; MCP, middle cerebellar peduncle; OR, optic radiation; P, posterior; R, right; SCP, superior cerebellar peduncle; SLF, superior longitudinal fasciculus; UF, uncinate fasciculus.

physiologies. Single-ventricle cardiac physiologies include cardiac defects where one ventricle is severely under-developed or the ventricular septal wall is absent, leaving a single functional ventricle, such as in the case of hypoplastic left heart syndrome. Two-ventricle physiologies encompass cardiac defects wherein both ventricles are preserved. This category includes dextro-transposition of the great arteries, in which the origin points of the pulmonary artery and the aorta are inverted, and tetralogy of Fallot, characterized by a combination of pulmonary stenosis, right ventricular hypertrophy, ventricular septal defect, and an overriding aorta. Given the clinical diversity of the CHD population, it can be expected that the severity and extent of myelination deficits may differ according to the severity of the specific cardiac defect.

Myelin deficits were most widespread and pronounced in youth with single-ventricle physiologies, with the highest range of effect sizes and the greatest number of affected tracts, including tracts in all four categories. We hypothesize that this pattern of more pronounced myelin deficits in the single-ventricle sub-group reflects the greater severity of single-ventricle cardiac defects. Compared to individuals with two-ventricle physiologies, those with single-ventricle cardiac physiologies typically present with greater hemodynamic instability and more pronounced disruptions to pre-operative cerebral blood flow (Cheng et al., 2020; Donofrio & Massaro, 2010; Nagaraj et al., 2015). As myelination deficits in the CHD population are proposed to occur secondary to cerebral hypoxia-ischemia, the greater disruption to cerebral blood flow in individuals with single-ventricle physiologies could theoretically also result in more pronounced myelination deficits in this sub-group. However, we have limited insight regarding the etiology of this finding considering the limited number of clinical factors we could extract from participants' medical records. Specifically, we were unable to extract factors directly related to perinatal cerebral blood flow and oxygenation for our cohort, as our participants were born in the 1990s and early 2000s before the advent of modern medical technologies that have facilitated the convenient monitoring and digital recording of hemodynamic factors.

Myelination deficits relative to controls were not limited to the single-ventricle sub-group and were also observed in participants with two-ventricle cardiac physiologies. Significant differences compared to controls were also observed in the dextro-transposition of the great arteries sub-group and the pooled other two-ventricle physiology sub-group, predominantly in association tracts and in the central corpus callosum. Interestingly, we did not observe any differences in our myelin measures between youth with tetralogy of Fallot and controls. In contrast with our findings, previous work has reported that brain development is indeed compromised in children and adolescents with tetralogy of Fallot, as seen by structural brain abnormalities and adverse neurodevelopmental and psychiatric outcomes (Bellinger et al., 2015; Kordopati-Zilou et al., 2022; Yang et al., 2022). When considering our sub-group analyses, it is important to note that the relatively small sample size of the diagnostic sub-groups may have limited the statistical power to detect group differences, and therefore, should be interpreted with caution. In particular, our null findings with respect to the tetralogy of Fallot sub-group should not be interpreted

as conclusive evidence of preserved myelination in youth with this cardiac defect. As such, future studies with tailored study design and strong statistical power to examine specific CHD diagnoses will provide greater insight into the differential risk of specific cardiac physiologies for myelination deficits and their functional impacts.

### 4.3 | Clinical implications of myelination deficits

Appropriate myelination of white matter tracts is critical in ensuring efficient signal transmission within brain networks (Fries, 2005), supporting a variety of cognitive, behavioral, and sensorimotor functions (Schmahmann et al., 2008). Consistent with this, early-life myelination, as measured by mcDESPOT-derived MWF, has been linked to the development of the cognitive abilities of healthy infants and children (Deoni et al., 2016; O'Muircheartaigh et al., 2014). Specific to the CHD population, previous diffusion tensor imaging studies have reported lower fractional anisotropy in youth with CHD to be associated with poorer outcomes in various cognitive domains, including memory, attention, and executive functioning (Brewster et al., 2015; Ehrler et al., 2020; Rollins et al., 2014; Watson et al., 2018). Thus, we can anticipate that the observed myelination disruptions, measured by MWF, may underlie the suboptimal cognitive, behavioral, and motor functioning frequently experienced by CHD survivors (Bolduc et al., 2020; Easson et al., 2019; Latal, 2016). In this line of thought, the more pronounced myelin deficits observed in youth with single-ventricle physiologies in the present study may be linked to the poorer neurodevelopmental outcomes documented in this vulnerable sub-group as compared to individuals with two-ventricle physiologies (Easson et al., 2019; Forbess et al., 2002).

In particular, we observed lower MWF in many association tracts and throughout the corpus callosum, which are believed to play a role in numerous higher-order cognitive functions such as language, learning and memory, attention and perception, visual-spatial processing, and emotional processing (Schmahmann et al., 2008). In addition, myelination deficits in the projection tracts could result in sensorimotor deficits. For example, the corticospinal tract, which connects cortical motor regions to lower motor neurons, could specifically be related to the gross and fine motor difficulties experienced by many CHD survivors (Bolduc et al., 2020).

Interestingly, previous diffusion tensor imaging studies have demonstrated that task training can potentially influence white matter microstructure, possibly including increased myelination, in healthy children, adolescents, and young adults (Bengtsson et al., 2005; Scholz et al., 2009). This suggests that MWF may be an interesting biomarker of intervention effectiveness in future trials, including trials of working memory training in youth with CHD (Calderon et al., 2020).

In the present study, we did not find evidence of significant relationships between our myelin measures and cognitive deficit or ADHD diagnosis. However, the small number of CHD participants in these sub-groups, and the potential presence of participants with undiagnosed ADHD in our sample, may have limited our ability to

detect significant associations. Furthermore, these dichotomous neurodevelopmental classifications may be less sensitive in detecting structure-function relationships as compared to standardized evaluations that provide continuous outcome scores, particularly with respect to examining the borderline or sub-clinical neurodevelopmental difficulties that may occur in this population (Easson et al., 2019). Future studies exploring specific structure-function relationships between myelination deficits and neuropsychological outcomes in individuals with CHD, employing comprehensive batteries of standardized cognitive, behavioral, and motor evaluations, will clarify the functional implications of our findings.

### 4.4 | Limitations

The findings of this study should be interpreted in the context of several limitations. Firstly, while MWF is strongly correlated with histological measurements of myelin content (Laule et al., 2006), it remains a proxy measure of myelination, as only histological studies can directly confirm myelin content. In addition, the mcDESPOT model is only able to produce a single MWF estimate per voxel, which poses a limitation given that up to 90% of voxels may contain multiple fiber populations in crossing configurations (Jeurissen et al., 2013). Consequently, deficient myelination in a given white matter tract may reduce average MWF estimates in unaffected tracts with which it intersects, therefore impacting our identification of regional myelination deficits in specific white matter tracts using tract-average MWF values. Additionally, we did not perform a fully battery of standardized cognitive, behavioral, or motor evaluations in our study, which limited our ability to determine the functional correlates of our findings. Furthermore, our CHD group was heterogenous, comprised of individuals with a variety of different single- and two-ventricle cardiac physiologies, preventing us from robustly examining specific CHD diagnoses with sufficient statistical power. Regardless, our heterogenous sample of complex CHD is representative of the clinical diversity of CHD, and therefore, our findings are generalizable to the true CHD population as a whole.

## 5 | CONCLUSION

In conclusion, this study provides specific evidence of widespread myelination deficits in youth born with CHD, confirming that brain dysmaturation in this population persists through early adulthood. Myelination deficits, as measured by MWF, were predominant in association tracts, projection tracts, and the corpus callosum, and were widespread and pronounced enough to be captured by a simple global summary measure, the White Matter Myelination Index. MWF has the potential to be a biomarker of myelination deficits and effectiveness of novel intervention strategies specific to the CHD population. Future structure-function investigations examining relationships between myelin deficits and the frequently reported cognitive,

behavioral, and motor difficulties experienced by CHD survivors are needed to confirm the functional significance of the reported myelin alterations.

## ACKNOWLEDGMENTS

First and foremost, we would like to thank the participants and their families for their participation in this study. We would also like to thank the MRI technologists, research coordinators, and research assistants at the ABCD Research Laboratory, and the clinicians at the McGill University Health Centre for their involvement in this project. We would particularly like to thank Dr. Pia Wintermark (Montreal Children's Hospital), Dr. Annette Majnemer (McGill University & Montreal Children's Hospital), and Jean Christophe-Houde (Université de Sherbrooke) for their expertise and advice. This research was enabled in part by support provided by Calcul Québec ([www.calculquebec.ca](http://www.calculquebec.ca)) and Compute Canada ([www.computeCanada.ca](http://www.computeCanada.ca)).

## CONFLICT OF INTEREST

The authors declare no competing interests.

## PATIENT CONSENT STATEMENT

Written informed consent was obtained from participants aged 18 years and older and from the legal guardians of participants aged younger than 18 years. Participants younger than 18 years also provided written informed assent.

## DATA AVAILABILITY STATEMENT

Data available on request from the authors.

## ORCID

Marie Brossard-Racine  <https://orcid.org/0000-0003-0641-0054>

## REFERENCES

- Axelrod, B. N. (2002). Validity of the Wechsler abbreviated scale of intelligence and other very short forms of estimating intellectual functioning. *Assessment*, 9(1), 17–23. <https://doi.org/10.1177/1073191102009001003>
- Back, S. A., Luo, N. L., Borenstein, N. S., Levine, J. M., Volpe, J. J., & Kinney, H. C. (2001). Late oligodendrocyte progenitors coincide with the developmental window of vulnerability for human perinatal white matter injury. *The Journal of Neuroscience*, 21(4), 1302–1312. <https://doi.org/10.1523/JNEUROSCI.21-04-01302.2001>
- Bellinger, D. C., Rivkin, M. J., DeMaso, D., Robertson, R. L., Stopp, C., Dunbar-Masterson, C., Wypij, D., & Newburger, J. W. (2015). Adolescents with tetralogy of Fallot: Neuropsychological assessment and structural brain imaging. *Cardiology in the Young*, 25(2), 338–347. <https://doi.org/10.1017/S1047951114000031>
- Bengtsson, S. L., Nagy, Z., Skare, S., Forsman, L., Forssberg, H., & Ullen, F. (2005). Extensive piano practicing has regionally specific effects on white matter development. *Nature Neuroscience*, 8(9), 1148–1150. <https://doi.org/10.1038/nn1516>
- Bolduc, M. E., Dionne, E., Gagnon, I., Rennick, J. E., Majnemer, A., & Brossard-Racine, M. (2020). Motor impairment in children with congenital heart defects: A systematic review. *Pediatrics*, 146(6), e20200083. <https://doi.org/10.1542/peds.2020-0083>
- Brewster, R. C., King, T. Z., Burns, T. G., Drossner, D. M., & Mahle, W. T. (2015). White matter integrity dissociates verbal memory and auditory attention span in emerging adults with congenital heart disease. *Journal of the International Neuropsychological Society*, 21(1), 22–33. <https://doi.org/10.1017/S135561771400109X>
- Brossard-Racine, M., du Plessis, A., Vezina, G., Robertson, R., Donofrio, M., Tworetzky, W., & Limperopoulos, C. (2016). Brain injury in neonates with complex congenital heart disease: What is the predictive value of MRI in the fetal period? *American Journal of Neuroradiology*, 37(7), 1338–1346. <https://doi.org/10.3174/ajnr.A4716>
- Calderon, J., Wypij, D., Rofeberg, V., Stopp, C., Roseman, A., Albers, D., Newburger, J. W., & Bellinger, D. C. (2020). Randomized controlled trial of working memory intervention in congenital heart disease. *The Journal of Pediatrics*, 227, 191–198. <https://doi.org/10.1016/j.jpeds.2020.08.038>
- Cheng, H. H., Ferradal, S. L., Vyas, R., Wigmore, D., McDavitt, E., Soul, J. S., Franceschini, M. A., Newburger, J. W., & Grant, P. E. (2020). Abnormalities in cerebral hemodynamics and changes with surgical intervention in neonates with congenital heart disease. *The Journal of Thoracic and Cardiovascular Surgery*, 159(5), 2012–2021. <https://doi.org/10.1016/j.jtcvs.2019.08.045>
- Cousineau, M., Jodoin, P. M., Morency, F. C., Rozanski, V., Grand'Maison, M., Bedell, B. J., & Descoteaux, M. (2017). A test-retest study on Parkinson's PPMI dataset yields statistically significant white matter fascicles. *NeuroImage: Clinical*, 16, 222–233. <https://doi.org/10.1016/j.nicl.2017.07.020>
- Dahan-Oliel, N., Mazer, B., Maltais, D. B., Riley, P., Nadeau, L., & Majnemer, A. (2014). Child and environmental factors associated with leisure participation in adolescents born extremely preterm. *Early Human Development*, 90(10), 665–672. <https://doi.org/10.1016/j.earlhumdev.2014.08.005>
- Deoni, S. C. L. (2011). Correction of main and transmit magnetic field (B0 and B1) inhomogeneity effects in multicomponent-driven equilibrium single-pulse observation of T1 and T2. *Magnetic Resonance in Medicine*, 65(4), 1021–1035. <https://doi.org/10.1002/mrm.22685>
- Deoni, S. C. L., Dean, D. C., 3rd, O'Muircheartaigh, J., Dirks, H., & Jersey, B. A. (2012). Investigating white matter development in infancy and early childhood using myelin water fraction and relaxation time mapping. *NeuroImage*, 63(3), 1038–1053. <https://doi.org/10.1016/j.neuroimage.2012.07.037>
- Deoni, S. C. L., Matthews, L., & Kolind, S. H. (2013). One component? Two components? Three? The effect of including a nonexchanging "free" water component in multicomponent driven equilibrium single pulse observation of T1 and T2. *Magnetic Resonance in Medicine*, 70(1), 147–154. <https://doi.org/10.1002/mrm.24429>
- Deoni, S. C. L., O'Muircheartaigh, J., Elison, J. T., Walker, L., Doernberg, E., Waskiewicz, N., Dirks, H., Piryatinsky, I., Dean, D. C., & Jumble, N. L. (2016). White matter maturation profiles through early childhood predict general cognitive ability. *Brain Structure & Function*, 221(2), 1189–1203. <https://doi.org/10.1007/s00429-014-0947-x>
- Deoni, S. C. L., Zinkstok, J. R., Daly, E., Ecker, C., Consortium, M. A., Williams, S. C., & Murphy, D. G. (2015). White-matter relaxation time and myelin water fraction differences in young adults with autism. *Psychological Medicine*, 45(4), 795–805. <https://doi.org/10.1017/S0033291714001858>
- Di Ciccio, C. J., & Romano, J. P. (2017). Robust permutation tests for correlation and regression coefficients. *Journal of the American Statistical Association*, 112(519), 1211–1200. <https://doi.org/10.1080/01621459.2016.1202117>
- Di Tommaso, P., Chatzou, M., Floden, E. W., Barja, P. P., Palumbo, E., & Notredame, C. (2017). Nextflow enables reproducible computational workflows. *Nature Biotechnology*, 35(4), 316–319. <https://doi.org/10.1038/nbt.3820>
- Donofrio, M. T., & Massaro, A. N. (2010). Impact of congenital heart disease on brain development and neurodevelopmental outcome. *International Journal Of Pediatrics*, 2010, 1–13. <https://doi.org/10.1155/2010/359390>
- Dumont, M., Roy, M., Jodoin, P. M., Morency, F. C., Houde, J. C., Xie, Z., Bauer, C., Samad, T. A., van Dijk, K., Goodman, J. A., Descoteaux, M., &

- Alzheimer's Disease Neuroimaging Initiative. (2019). Free water in white matter differentiates MCI and AD from control subjects. *Frontiers in Aging Neuroscience*, 11, 270. <https://doi.org/10.3389/fnagi.2019.00270>
- Dvorak, A. V., Swift-LaPointe, T., Vavasour, I. M., Lee, L. E., Abel, S., Russell-Schulz, B., Graf, C., Wurl, A., Liu, H., Laule, C., Li, D. K. B., Traboulsee, A., Tam, R., Boyd, L. A., MacKay, A., & Kolind, S. H. (2021). An atlas for human brain myelin content throughout the adult life span. *Scientific Reports*, 11(1), 269. <https://doi.org/10.1038/s41598-020-79540-3>
- Easson, K., Dahan-Oliel, N., Rohlicek, C., Sahakian, S., Brossard-Racine, M., Mazer, B., Riley, P., Maltais, D. B., Nadeau, L., Hatzigeorgiou, S., Schmitz, N., & Majnemer, A. (2019). A comparison of developmental outcomes of adolescent neonatal intensive care unit survivors born with a congenital heart defect or born preterm. *The Journal of Pediatrics*, 207, 34–41. <https://doi.org/10.1016/j.jpeds.2018.11.002>
- Easson, K., Rohlicek, C. V., Houde, J. C., Gilbert, G., Saint-Martin, C., Fontes, K., Majnemer, A., Marelli, A., Wintermark, P., Descoteaux, M., & Brossard-Racine, M. (2020). Quantification of apparent axon density and orientation dispersion in the white matter of youth born with congenital heart disease. *NeuroImage*, 205, 116255. <https://doi.org/10.1016/j.neuroimage.2019.116255>
- Ehrler, M., Latal, B., Kretschmar, O., von Rhein, M., & O'Gorman Tuura, R. (2020). Altered frontal white matter microstructure is associated with working memory impairments in adolescents with congenital heart disease: A diffusion tensor imaging study. *NeuroImage: Clinical*, 25, 102123. <https://doi.org/10.1016/j.nicl.2019.102123>
- Fontes, K., Rohlicek, C. V., Saint-Martin, C., Gilbert, G., Easson, K., Majnemer, A., Marelli, A., Chakravarty, M. M., & Brossard-Racine, M. (2019). Hippocampal alterations and functional correlates in adolescents and young adults with congenital heart disease. *Human Brain Mapping*, 40, 3548–3560. <https://doi.org/10.1002/hbm.24615>
- Forbess, J. M., Visconti, K. J., Hancock-Friesen, C., Howe, R. C., Bellinger, D. C., & Jonas, R. A. (2002). Neurodevelopmental outcome after congenital heart surgery: Results from an institutional registry. *Circulation*, 106(12 Suppl 1), I95–I102. <https://doi.org/10.1161/01.cir.0000032915.33237.72>
- Fries, P. (2005). A mechanism for cognitive dynamics: Neuronal communication through neuronal coherence. *Trends in Cognitive Sciences*, 9(10), 474–480. <https://doi.org/10.1016/j.tics.2005.08.011>
- Garyfallidis, E., Côté, M. A., Rheault, F., Sidhu, J., Hau, J., Petit, L., Fortin, D., Cunanne, S., & Descoteaux, M. (2018). Recognition of white matter bundles using local and global streamline-based registration and clustering. *NeuroImage*, 170, 283–295. <https://doi.org/10.1016/j.neuroimage.2017.07.015>
- Hollingshead, A. B. (2011). Four factor index of social status. *Yale Journal of Sociology*, 8, 21–51.
- Hooper, V. S., & Bell, S. M. (2006). Concurrent validity of the universal nonverbal intelligence test and the Leiter international performance scale—revised. *Psychology in the Schools*, 43(2), 17–23. <https://doi.org/10.1002/pits.20136>
- Jeurissen, B., Leemans, A., Tournier, J. D., Jones, D. K., & Sijbers, J. (2013). Investigating the prevalence of complex fiber configurations in white matter tissue with diffusion magnetic resonance imaging. *Human Brain Mapping*, 34(11), 2747–2766. <https://doi.org/10.1002/hbm.22099>
- Jones, D. K., Knosche, T. R., & Turner, R. (2013). White matter integrity, fiber count, and other fallacies: The do's and don'ts of diffusion MRI. *NeuroImage*, 73, 239–254. <https://doi.org/10.1016/j.neuroimage.2012.06.081>
- Karmacharya, S., Gagoski, B., Ning, L., Vyas, R., Cheng, H. H., Soul, J., Newburger, J. W., Shenton, M. E., Rath, Y., & Grant, P. E. (2018). Advanced diffusion imaging for assessing normal white matter development in neonates and characterizing aberrant development in congenital heart disease. *NeuroImage: Clinical*, 19, 360–373. <https://doi.org/10.1016/j.nicl.2018.04.032>
- Kinney, H. C., Panigrahy, A., Newburger, J. W., Jonas, R. A., & Sleeper, L. A. (2005). Hypoxic-ischemic brain injury in infants with congenital heart disease dying after cardiac surgery. *Acta Neuropathologica*, 110(6), 563–578. <https://doi.org/10.1007/s00401-005-1077-6>
- Kordopati-Zilou, K., Sergentanis, T., Pervanidou, P., Sofianou-Petraki, D., Panoulis, K., Vlahos, N., & Eleftheriades, M. (2022). Neurodevelopmental outcomes in tetralogy of Fallot: A systematic review. *Children (Basel)*, 9(2), 264. <https://doi.org/10.3390/children9020264>
- Kurtzer, G. M., Sochat, V., & Bauer, M. W. (2017). Singularity: Scientific containers for mobility of compute. *PLoS One*, 12(5), e0177459. <https://doi.org/10.1371/journal.pone.0177459>
- Latal, B. (2016). Neurodevelopmental outcomes of the child with congenital heart disease. *Clinics in Perinatology*, 43(1), 173–185. <https://doi.org/10.1016/j.clp.2015.11.012>
- Laule, C., Leung, E., Lis, D. K., Traboulsee, A. L., Paty, D. W., MacKay, A. L., & Moore, G. R. (2006). Myelin water imaging in multiple sclerosis: Quantitative correlations with histopathology. *Multiple Sclerosis*, 12(6), 747–753. <https://doi.org/10.1177/1352458506070928>
- Lebel, C., & Beaulieu, C. (2011). Longitudinal development of human brain wiring continues from childhood into adulthood. *The Journal of Neuroscience*, 31(30), 10937–10947. <https://doi.org/10.1523/JNEUROSCI.5302-10.2011>
- Licht, D. J., Shera, D. M., Clancy, R. R., Wernovsky, G., Montenegro, L. M., Nicolson, S. C., Zimmerman, R. A., Spray, T. L., Gaynor, J. W., & Vossough, A. (2009). Brain maturation is delayed in infants with complex congenital heart defects. *The Journal of Thoracic and Cardiovascular Surgery*, 137(3), 529–537. <https://doi.org/10.1016/j.jtcvs.2008.10.025>
- Licht, D. J., Wang, J., Silvestre, D. W., Nicolson, S. C., Montenegro, L. M., Wernovsky, G., Tabbutt, S., Durning, S. M., Shera, D. M., Gaynor, J. W., Spray, T. L., Clancy, R. R., Zimmerman, R. A., & Detre, J. A. (2004). Preoperative cerebral blood flow is diminished in neonates with severe congenital heart defects. *The Journal of Thoracic and Cardiovascular Surgery*, 128(6), 841–849. <https://doi.org/10.1016/j.jtcvs.2004.07.022>
- Limperopoulos, C., Tworetzky, W., McElhinney, D. B., Newburger, J. W., Brown, D. W., Robertson, R. L., Guizard, N., McGrath, E., Geva, J., Annese, D., Dunbar-Masterson, C., Trainor, B., Laussen, P. C., & du Plessis, A. J. (2010). Brain volume and metabolism in fetuses with congenital heart disease: Evaluation with quantitative magnetic resonance imaging and spectroscopy. *Circulation*, 121(1), 26–33. <https://doi.org/10.1161/CIRCULATIONAHA.109.865568>
- Mahle, W. T., Tavani, F., Zimmerman, R. A., Nicolson, S. C., Galli, K. K., Gaynor, J. W., Clancy, R. R., Montenegro, L. M., Spray, T. L., Chiavacci, R. M., Wernovsky, G., & Kurth, C. D. (2002). An MRI study of neurological injury before and after congenital heart surgery. *Circulation*, 106(12 Suppl 1), I109–I114. <https://doi.org/10.1161/01.cir.0000032908.33237.b1>
- Miller, S. P., McQuillen, P. S., Hamrick, S., Xu, D., Glidden, D. V., Charlton, N., Karl, T., Azakie, A., Ferriero, D. M., Barkovich, A. J., & Vigneron, D. B. (2007). Abnormal brain development in newborns with congenital heart disease. *The New England Journal of Medicine*, 357(19), 1928–1938. <https://doi.org/10.1056/NEJMoa067393>
- Miller, S. P., McQuillen, P. S., Vigneron, D. B., Glidden, D. V., Barkovich, A. J., Ferriero, D. M., Hamrick, S. E. G., Azakie, A., & Karl, T. R. (2004). Preoperative brain injury in newborns with transposition of the great arteries. *The Annals of Thoracic Surgery*, 77(5), 1698–1706. <https://doi.org/10.1016/j.athoracsur.2003.10.084>
- Morris, S. R., Holmes, R. D., Dvorak, A. V., Liu, H., Yoo, Y., Vavasour, I. M., Mazabel, S., Mädler, B., Kolind, S. H., Li, D. K. B., Siegel, L., Beaulieu, C., MacKay, A. L., & Laule, C. (2020). Brain myelin water fraction and diffusion tensor imaging atlases for 9–10 year-old children. *Journal of Neuroimaging*, 30(2), 150–160. <https://doi.org/10.1111/jon.12689>

- Morton, P. D., Ishibashi, N., & Jonas, R. A. (2017). Neurodevelopmental abnormalities and congenital heart disease: Insights into altered brain maturation. *Circulation Research*, 120(6), 960–977. <https://doi.org/10.1161/CIRCRESAHA.116.309048>
- Nagaraj, U. D., Evangelou, I. E., Donofrio, M. T., Vezina, L. G., McCarter, R., du Plessis, A. J., & Limperopoulos, C. (2015). Impaired global and regional cerebral perfusion in newborns with complex congenital heart disease. *The Journal of Pediatrics*, 167(5), 1018–1024. <https://doi.org/10.1016/j.jpeds.2015.08.004>
- Nichols, T. E., & Holmes, A. P. (2002). Nonparametric permutation tests for functional neuroimaging: A primer with examples. *Human Brain Mapping*, 15(1), 1–25. <https://doi.org/10.1002/hbm.1058>
- O'Muircheartaigh, J., Dean D. C., 3rd, Ginestet, C. E., Walker, L., Waskiewicz, N., Lehman, K., Dirks, H., Piryatinsky, I., & Deoni, S. C. L. (2014). White matter development and early cognition in babies and toddlers. *Human Brain Mapping*, 35(9), 4475–4487. <https://doi.org/10.1002/hbm.22488>
- Rivkin, M. J., Watson, C. G., Scoppettuolo, L. A., Wypij, D., Vajapeyam, S., Bellinger, D. C., DeMaso, D., Robertson, R. L., & Newburger, J. W. (2013). Adolescents with D-transposition of the great arteries repaired in early infancy demonstrate reduced white matter microstructure associated with clinical risk factors. *The Journal of Thoracic and Cardiovascular Surgery*, 146(3), 543–549.e1. <https://doi.org/10.1016/j.jtcvs.2012.12.006>
- Roid, G. H., & Miller, L. J. (2011). *Leiter international performance scale-revised (Leiter-R)*. Psymtec.
- Rollins, C. K., Watson, C. G., Asaro, L. A., Wypij, D., Vajapeyam, S., Bellinger, D. C., DeMaso, D., Robertson, R. L., Newburger, J. W., & Rivkin, M. J. (2014). White matter microstructure and cognition in adolescents with congenital heart disease. *The Journal of Pediatrics*, 165(5), 936–944. <https://doi.org/10.1016/j.jpeds.2014.07.028>
- Ryan, J. J., Carruthers, C. A., Miller, L. J., Souheaver, G. T., Gontkovsky, S. T., & Zehr, M. D. (2003). Exploratory factor analysis of the Wechsler Abbreviated Scale of Intelligence (WASI) in adult standardization and clinical samples. *Applied Neuropsychology*, 10(4), 252–256. [https://doi.org/10.1207/s15324826an1004\\_8](https://doi.org/10.1207/s15324826an1004_8)
- Saklofske, D. H., Caravan, G., & Schwartz, C. (2000). Concurrent validity of the Wechsler Abbreviated Scale of Intelligence (WASI) with a sample of Canadian children. *Canadian Journal of School Psychology*, 16(1), 87–94. <https://doi.org/10.1177/082957350001600106>
- Schmahmann, J. D., Smith, E. E., Eichler, F. S., & Filley, C. M. (2008). Cerebral white matter: Neuroanatomy, clinical neurology, and neurobehavioral correlates. *Annals of the New York Academy of Sciences*, 1142, 266–309. <https://doi.org/10.1196/annals.1444.017>
- Scholz, J., Klein, M. C., Behrens, T. E., & Johansen-Berg, H. (2009). Training induces changes in white-matter architecture. *Nature Neuroscience*, 12(11), 1370–1371. <https://doi.org/10.1038/nn.2412>
- Spader, H. S., Dean, D. C., 3rd, LaFrance, W. C., Raukar, N. P., Cosgrove, G. R., Eyerly-Webb, S. A., Ellermeier, A., Correia, S., Deoni, S. C. L., & Rogg, J. (2018). Prospective study of myelin water fraction changes after mild traumatic brain injury in collegiate contact sports. *Journal of Neurosurgery*, 130(4), 1–9. <https://doi.org/10.3171/2017.12.JNS171597>
- Sun, L., Macgowan, C. K., Sled, J. G., Yoo, S. J., Manlhiot, C., Porayette, P., Grosse-Wortmann, L., Jaeggi, E., McCrindle, B., Kingdom, J., Hickey, E., Miller, S., & Seed, M. (2015). Reduced fetal cerebral oxygen consumption is associated with smaller brain size in fetuses with congenital heart disease. *Circulation*, 131(15), 1313–1323. <https://doi.org/10.1161/CIRCULATIONAHA.114.013051>
- Theaud, G., Houde, J. C., Bore, A., Rheault, F., Morency, F., & Descoteaux, M. (2020). TractoFlow: A robust, efficient and reproducible diffusion MRI pipeline leveraging Nextflow & Singularity. *NeuroImage*, 218, 116889. <https://doi.org/10.1016/j.neuroimage.2020.116889>
- Watson, C. G., Stopp, C., Wypij, D., Bellinger, D. C., Newburger, J. W., & Rivkin, M. J. (2018). Altered white matter microstructure correlates with IQ and processing speed in children and adolescents post-Fontan. *The Journal of Pediatrics*, 200, 140–149. <https://doi.org/10.1016/j.jpeds.2018.04.022>
- Wechsler, D. (1999). *Wechsler abbreviated scale of intelligence*. The Psychological Corporation: Harcourt Brace & Company.
- Yang, M., Liu, Y., Ma, S., Wang, S., Fu, M., Zhu, M., Li, Y., Cheng, S., Feng, Z., Yang, M., & Mo, X. (2022). Altered brain structure in preschool-aged children with tetralogy of Fallot. *Pediatric Research*. Advance online publication. <https://doi.org/10.1038/s41390-022-01987-z>

**How to cite this article:** Easson, K., Gilbert, G., Rohlicek, C. V., Saint-Martin, C., Descoteaux, M., Deoni, S. C. L., & Brossard-Racine, M. (2022). Altered myelination in youth born with congenital heart disease. *Human Brain Mapping*, 43(11), 3545–3558. <https://doi.org/10.1002/hbm.25866>